

Published in: *Visual Cognition*, vol. 25, pp. 169-183

(Iss. 1-3: The Visual Mind - A Special issue in Honor of Glyn W. Humphreys)

Pathological completion in the intact visual field of hemianopia patients

Galina V. Paramei^{a*}, Ophélie Favrod^{b*}, Bernhard A. Sabel^c & Michael H. Herzog^b

^a Department of Psychology, Liverpool Hope University, Liverpool, UK;

^b Laboratory of Psychophysics, Brain Mind Institute, École Polytechnique Fédérale de Lausanne (EPFL), Lausanne, Switzerland

^c Institute of Medical Psychology, Otto-von-Guericke University of Magdeburg, Magdeburg, Germany

Corresponding author:

Galina V. Paramei

Email: parameg@hope.ac.uk

Department of Psychology

Liverpool Hope University

Hope Park

L16 9JD Liverpool

United Kingdom

RUNNING HEAD: Hemianopia patients' intact visual field

*Both Authors contributed equally to the study

Abstract

We investigated figure segregation in the intact visual field (VF) of hemianopia patients. Three patients and matched controls performed a Yes–No figure detection task, where square or square fragments were embedded in a background of randomly oriented Gabor elements. We varied orientation and number of the fragment elements, stimulus eccentricity and background density (BD). Figure detection was impaired in all three patients in the entire intact VF, but potentially more pronounced in patients with cortical lesions. “Pathological completion” was most frequently observed for high BDs and for square fragments oriented towards the blind hemifield. Our findings confirm contour integration deficits in the intact VF of hemianopia patients. Further, our results indicate that (1) contour integration deficits are exacerbated by contextual interaction and (2) “pathological completion” appears to be more likely associated with lesions of cortical rather than geniculo-striate origin. The deficits point to increased lateral suppressive inputs from background elements.

Key words: hemianopia; intact visual field; contour integration; pathological completion; contextual interaction

Introduction

Homonymous hemianopia is defined as bilateral blindness in a visual hemifield, caused by retrochiasmal lesions within the geniculo-striate pathways contralateral to the site of the lesion (for a review see Chokron, Perez, & Peyrin, 2016). Surprisingly, even the ipsilateral “intact” hemifield can reveal subtle deficits of visual processing. Standard methods of visual field testing, perimetry or campimetry, tackle the loss of visual *sensation* in the blind hemifield but fail to capture deficits in the intact visual field (VF).

In a pioneering study, Poppelreuter (1917/1990) found that when presented with complex stimuli, hemianopic patients with occipital and parietal lesions (of World War I occiput injuries) manifested degraded perception beyond the perimetrically blind hemifield. A similar finding motivated Fuchs (1920) to introduce a classic distinction between the patient’s perimetric field (*Gesichtsfeld*) and the field of actual vision (*Sehfeld*). Recently this phenomenon was coined *sightblindness* (Bola, Gall, & Sabel, 2013a).

Deficits in the ipsilateral “intact” hemifield of hemianopic patients are elevated contrast thresholds (Hess & Pointer, 1989), compromised detection of a signal surrounded by distracters and pathological reduction of the useful field of view, indicating diminished visual attention capacity (Rizzo & Robin, 1996). Bender and Teuber (1946) reported that hemianopic patients often complain that their vision is “too slow”. The finding was confirmed in recent studies (Bola, Gall, & Sabel, 2013b; Cavézian et al., 2010, 2015; Geuzebroek & van den Berg, 2017; Poggel, Treutwein, & Strasburger, 2011; Rizzo & Robin, 1996).

In a previous report (Paramei & Sabel, 2008), we demonstrated that detection of a figure embedded in a noisy background is deteriorated in the intact VF of hemianopic patients with cortical lesions. For a patient with optic tract lesion, we found no such deficit. A follow-up study using EEG (Schadow et al., 2009) showed that, compared to healthy controls, in hemianopic patients, gamma-band responses to Gestalt-like patterns were attenuated between 200 and 400 ms after stimulus onset, indicating deficits in both early and late visual processing.

These findings indicate deficient spatial and temporal integration of hemianopia patients’ “intact” hemifield. Notably, besides diminished visual processing, i.e., a “hypofunction”, these patients reveal a “hyperfunction” manifested by the phenomenon of “pathological completion”, described by Poppelreuter (1917/1990) with the term later coined by Walker and Mattingley (1997; see also Mattingley & Walker, 2003). Under certain conditions incomplete images presented foveally, involving both the intact and blind hemifield, are “completed”. Several studies reported that, when presented with half of the figure entirely within the intact hemifield such that its edges are abutting to the border of the blind hemifield, hemianopes quite often report the figure as a whole (Bender & Teuber, 1946; Fuchs, 1920; McCarthy, James-Galton, & Plant, 2006; Sergent, 1988; Warrington, 1962, 1965; Weil, Plant, James-Galton, & Rees, 2009).

The “completion” phenomenon is not due to unstable fixation, i.e., involuntary eye movements, which occasionally carry the image into the intact hemifield. No systematic differences were found in mean eye position across trials with veridical and pathological completion, either in the horizontal or vertical dimension (Weil et al., 2009). The studies with eye-tracking demonstrated

conclusively that “completion” is the genuine phenomenon and cannot be attributed to artefacts. It is influenced, though, by the capacity to achieve and maintain accurate fixation (Gassel & Williams, 1963) and/or fixation in the direction of a blind hemifield (Sergent, 1988).

Pathological completion is a recurrent observation that it is typical for hemianopic patients with occipital and parietal lesions (Poppelreuter, 1917/1990; Warrington, 1962, 1965), which points to the role of the lesion location upstream in the visual system. Depending on the location, the lesion causes perception deficits in the entire VF.

Certain conditions of occurrence of pathological completion in hemianopia patients are worth noting in relation to our findings reported below. First, both veridical and pathological completion can be elicited only with simple, regular and bilaterally symmetrical figures, such as circle, square or ellipse (Fuchs, 1920, 1921/1938; Marcel, 1998; Sergent, 1988; Torjussen, 1978). Second, high predictability of stimuli from their incomplete shape is critical for pathological completion (Poppelreuter, 1917/1990; Sergent, 1988). It is boosted when the awareness of the nature of stimuli and a verbal cue is provided (e.g., “circle”; Pollack, Battersby, & Bender, 1957). Third, complex meaningful figures (e.g., a flower, face) that are characterized by neither symmetry nor “goodness” in the Gestalt sense can be “completed” too, provided they depict objects which are familiar and readily named (Warrington, 1962, 1965). Fourth, completion is more likely with brief exposures (20–100 ms) rather than with longer exposures, up to 1 s (Bender & Teuber, 1946). With exposures longer than these, pathological completion disappears (Torjussen, 1978). These findings suggest that, at a brief exposure, a figure and its parts are explored insufficiently in hemianopic patients, whose perceptual decisions are based on partially available information.

Humphreys’ numerous careful and insight case studies of neuropsychological deficits of visual functions, in the first row of agnosia and neglect, are indispensable for current multi-stage account of binding (Humphreys, 2001, 2003) and contributed significantly to understanding of mechanisms of fundamental vision processes, such as grouping (Gilchrist, Humphreys, & Riddoch, 1996; Han, & Humphreys, 2007), figure-ground segregation (Giersch, Humphreys, Boucart, & Kovács, 2000), and contour integration (Vancleef, Wagemans, & Humphreys, 2013).

Here, to gain further insight into the mechanisms underlying figure recognition in hemianopic patients, we used arrays made of Gabor elements (GEs), which are locally oriented and also spatially band-passed (Field, Hayes, & Hess, 1993). These stimuli are well suited to tackle collinear facilitatory interactions between elements of the contour and their integration and segregation from a complex noisy background (Kovács & Julesz, 1993; Polat & Bonnet, 2000). We probed the grouping of non-contiguous elements in hemianopia patients in their intact hemifield, asking whether local integration affects their global contour integration required for correct figure recognition. Specifically, we presented either a figure (square), its fragments or the random background only.

In addition, to investigate contextual interactions, we varied the density of background elements, which defines the contour signal-to-noise ratio (see Kovács, Polat, Pennefather, Chandna, & Norcia, 2000). The choice of stimuli with varying degree of noisy background was motivated by the observation that hemianopes feel uncertain in crowded places (Gassel & Williams, 1963). By

increasing the signal-to-noise ratio, we explored how “contextual interactions” affect hemianopes’ ability of global figure segregation.

Furthermore, we tested whether figure fragments would be “completed” when presented not centrally, contiguous to the vertical midline, but entirely within either the affected or “intact” hemifield. The rationale was to test whether pathological completion manifests itself by ignoring of a missing portion of information or, rather, extrapolation of a presented portion of information. In addition, we explored the effect of eccentricity on the “completion”.

The current report is an extension of a previous publication (Paramei & Sabel, 2008), where we reported hemianopia patients’ and controls’ performance for square detection vs. random background for two extreme background densities, 0.5 and 1.0. Here the same participants’ performance is analysed, in addition, for square “detection” (pathological completion) when they were exposed to square fragments and, further, for four intermediate background densities (0.6–0.9). As measures of perceptual performance, hit rates, false alarms (FA) and RTs were analysed for the hemianopia patients in relation to those of the matched healthy controls.

Materials and Methods

Methods are described in more detail in Paramei and Sabel (2008). Here we briefly reiterate information on the participants and the procedure.

Participants

Three patients with homonymous hemianopia participated in the study.

- Patient **FJ** (male, 48 years old) manifested **left dense complete homonymous hemianopia**. The lesion resulted from surgery for tumour removal. The lesion mainly comprised anterior parts of the right inferior occipital and temporal lobes, with an upward extension to the anterior parietal cortex. The key structures of the geniculo-striate projections, lateral geniculate nucleus (LGN) and optical radiation, were also damaged. The splenium of the corpus callosum appeared to have remained intact and large areas of the primary visual cortex were still present. We classified the lesion as **occipital-parietal**, i.e., of **cortical** origin.
- Patient **HF** (male, 72 years old), with **left incomplete homonymous hemianopia**, with the left bottom quadrant greatly spared; sustained infarction of the right posterior cerebral artery. We classified the lesion as **occipital**, i.e., of **cortical** origin.
- Patient **UP** (female, 53 years old), with **right complete homonymous hemianopia**, had a pre-geniculate lesion: she suffered a closed head injury affecting her left optic tract. We classified the lesion as **pre-geniculate, optic tract**.

All patients had binocular vision with corrected acuity of 0.8 or better; none of them showed unilateral visual neglect (indicated by the line-bisection task).

- Three controls matched to the patients in age and gender participated in the study. All had normal or corrected-to-normal visual acuity and declared to have no visually related complaints.

Both patients and controls gave informed consent before participating. The study was approved by the Ethics Committee of the Institute of Medical Psychology, Otto-von-Guericke University of Magdeburg, and carried out in accordance with the Declaration of Helsinki.

Assessment of hemianopia patients' visual field

Prior to the experiment on figure detection, each hemianopia patient underwent low resolution perimetry using the Tübingen Automatic perimeter under monocular condition. In addition, each patient's VF was assessed using a computer-assisted high resolution perimetry (technically a campimetric method) under binocular viewing. For further patients' details and their low- and high-resolution perimetry outcomes see Table 1 and Figures 2 and 3 in Paramei and Sabel (2008).

Apparatus

Stimuli were presented on a 17-inch Eizo FlexScan L565 monitor with a 60 Hz refresh rate. It was controlled by a Megware microcomputer equipped with a Matrox Millennium G550 high-speed graphics card. At a viewing distance of 30 cm, the screen dimensions were 58° x 48° horizontally and vertically, respectively; the viewing area contained 1024 x 768 pixels. Stimulus luminance was measured by Mavo-Monitor (Gossen) photometer. Participant's head was stabilized with a chin and forehead rest. Each participant's position was adjusted to attain termination of the gaze line at the centrally displayed dim red fixation point. The room was otherwise darkened.

Stimuli

The target stimulus was a square (or a square fragment) composed of aligned GEs embedded in a background of randomly oriented GEs. Each GE consisted of a sinusoidal contrast modulation convolved with a Gaussian function, which matches optimally receptive-field properties of neurons in V1 (Field et al., 1993). GE parameters were as follows (see Braun, 1999): spatial period $\lambda=0.647^\circ$; phase $\varphi=0$; visual size= 1.2° ; minimal and maximal luminance at 0.4 cd/m^2 and 123 cd/m^2 , respectively, with contrast of 100%. The GEs were presented against a homogeneous grey background with a luminance of 32 cd/m^2 ; the latter was also shown between trials.

The entire VF (50°) was filled with randomly oriented GEs with some of them forming a target square (or square fragment) at one of 19 possible locations (Figure 1(a)).

Figure and fragment locations varied with regards to (1) one of six radii originating from the fixation point, with the separating angle of 60° , and (2) eccentricity, with values of 0° , 5° , 10° , and 15° along the radius. The total number of locations amounted to 19. Note that squares were presented at the centre. The grid of a (virtual) figure centres is shown in Figure 1(a). Here angular eccentricity in the right hemifield is depicted as positive and in the left hemifield as negative.

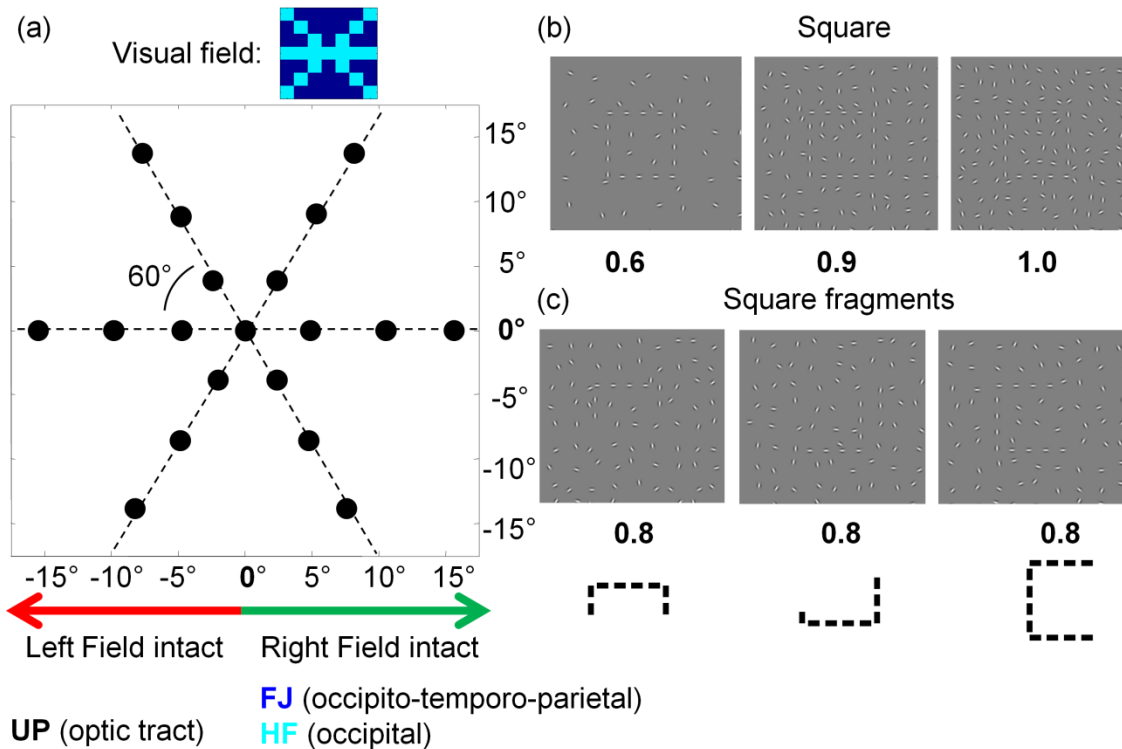


Figure 1. (a) Visual field representation. In polar coordinates, 19 locations of the centre of a square or square fragment are shown by black dots in the main panel (true location) and in light blue in the inset (schematic for the display purpose). The centre, 0° , is the fovea. Angular distance between each radius is 60° . The numbers underneath the main panel, $|5^\circ|$, $|10^\circ|$ and $|15^\circ|$, indicate eccentricity (deg) from the fovea along the six radii. (b) Examples of a square (target) embedded in three background densities. Noise increases from left to right. (c) Examples of square fragments with varying orientation and number of Gabor elements (from left to right: 8 symmetric, 8 asymmetric and 12 symmetric); background density 0.8. The square fragments are schematically presented by black dashed-line segments underneath the figure. Here fragment edges are oriented to the bottom, top or right, respectively.

Three categories of stimuli were randomly presented:

1. The target figure was a square of a size of 10.2° of visual angle, with contours comprised by collinear GEs (Figure 1(b)). The spacing between the contour elements was set to be equal to the length of the GE (1.2°). The square was embedded within an array of randomly oriented distracter GEs of the same spatial frequency, contrast, and uniform density.
2. To test false positives of figure detection, or pathological completion, fragments of square contour, with at least one corner, were presented. The number of different fragment versions amounted to 20, as a combination of the varying number of GEs and fragment orthogonal orientation. Specifically, the fragments were composed of either 4 GEs ($N=4$), 8 GEs ($N=12$) or 12 GEs ($N=4$). The 8-GE fragments were either symmetric or asymmetric;

these and the 12-GE fragments took one of two vertical or two horizontal modal orientations. Exemplary square fragments are shown in Figure 1(c); for full set of the square fragments see Figure S1 in Supplemental data.

3. Random arrays of GEs were used as catch trials also for probing pathological completion.

Background density (BD) of GEs was varied between runs; it changed the signal-to-noise ratio and, hence, visibility of the contour (Figure 1(b)). Following Kovács et al. (2000), the BD was defined as the ratio of the spacing between GEs constituting the target relative to the mean background GE spacing. In the present study, six BD values were employed: BD=0.5 corresponded to high visibility of the contour, with the spacing between the background GEs twice (sparser) the spacing between the GEs constituting the contour of a square or a fragment. Four intermediate BDs were employed: 0.6, 0.7, 0.8 and 0.9. Finally, BD=1.0 was the condition of a noisy background, i.e., poor contour visibility, whereby the spacing was equal between GEs in both the contour and the background.

Duration of stimuli

In a pilot experiment, it was found that reasonable performance levels of healthy controls were achieved for 200 ms exposure. In contrast, hemianopia patients required 500 ms exposure to enable above-chance performance, suggesting a compromised temporal processing (see Geuzebroek & van den Berg, 2017). Hence, stimulus duration was set to 500 ms for both controls and hemianopia patients. For both groups, the pre-stimulus interval was randomly varied between 1000 ms and 1500 ms. Post-stimulus interval was set for 2500 ms to accommodate the frequently observed motor deceleration compared to the controls.

Task

Participants were informed that either a square, a square fragment, or only the background will be presented. Their task was to report whether the square was present (Yes); absent (No), or if a square fragment was present (No), by pressing the right or left response keys, respectively, of a response box. Participants were instructed to respond as quickly as possible but also as accurately as possible. No feedback was provided. Prior to the experiment, participants performed several practice trials to familiarize themselves with the stimuli and the task.

Procedure

Participants were required to maintain strict fixation of the central point during stimulus presentation. Eye movements were not registered. None of the participants had any measurable fixation problem: a deviation of at most 1° from the fixation point was detected by the experimenter (GVP) who viewed the participant's eye position in a mirror during the trial.

A total of 600 trials were presented to the patients and healthy controls. One run consisted of 60 randomly interleaved trials: 20 trials with a square, 20 with random background and 20 with square fragments, each version presented once. Within a given run, BD was kept constant; stimuli were presented once at each VF location and twice in the central location. Each of six BDs was tested 10 times. Within a run, the high-visible condition (BD=0.5) was presented first, followed by five less-visible conditions (BD=0.6–1.0). Data collection was spread over several days, with a

maximum of 2-3 runs per day (depending the participant's level of fatigue and concentration). Correctness of responses and RTs were recorded.

Data analysis

Data were analysed using MATLAB (R2010b, The MathWorks Inc., Natick, MA). Invalid trials (e.g., timeout) were excluded from any further analysis.

For the trials with the square present, hit rate was estimated separately for the fovea stimulus location and beyond it for the patient's entire intact hemifield for each of the six BDs. A similar procedure was applied to the matched control. Note that the responses were pooled over nine non-central VF locations, i.e., those that implicated objective visibility of the (entire) square and, hence, veridical figure detection. For the trials with the background only display, FA rate was computed. The d' and the criterion C were also calculated. The two measures were corrected for extreme values (Hautus, 1995).

For square fragments, FA rate was computed separately for each of the 19 VF locations (i.e., both blind and intact VF). To explore whether certain fragment orientation is more likely to trigger "completion", only square fragments oriented either to the left or to the right were considered (see in Supplemental data Figure S1, Nos. 1-4, 6, 8, 10, 12, 14, 16, 18 and 20) but not fragments oriented either to the top or to the bottom. We defined a "Completion Orientation Index" (COI) as the difference between the FA rate for right- and left-oriented fragments. The COI was calculated for each VF location. Statistics were performed using JASP (Version 0.7.1.2 and 0.8.1.1).

Reaction times, averaged across all BDs, were analysed separately for the fovea and, beyond it, the entire intact hemifield. In addition, for correct square detection, RTs were pooled over the six BDs, as a function of the eccentricity in the intact hemifield. For correct rejection in the background only trials, RT histograms were obtained for each BD. RTs for square fragments are presented as Supplemental data (Table S1) since the repetition number for each fragment version per BD and VF location was too low ($N=10$) to allow a reliable estimation of the response speed.

Results

Figure detection: background density and contextual interaction

In accordance with our previous finding (Paramei & Sabel, 2008), figure detection in terms of hit rate decreased with increasing BD for all three patients, as shown in Figure 2(a) for the foveally presented squares (0°) and Figure 2(b) for the intact hemifield (with 0° -centred squares excluded). We carried out a repeated-measures ANOVA for the hit rate, with the "group" (patients vs. controls) and BD as factors. We found significant main effect of BD ($F(5,20)=24.356$, $p<.001$, $\eta^2=0.763$, with Greenhouse-Geisser corrected: $F(1.544, 6.174)=24.356$, $p=.002$, $\eta^2=0.763$). Surprisingly, the main effect of group was not significant ($F(1,4)=4.137$, $p=.112$, $\eta^2=0.508$), which may be explained by the heterogeneity of the two groups. Also significant was the interaction effect between the group and BD ($F(5,20)=3.583$, $p=.018$, $\eta^2=0.112$), however, when corrected for violation of sphericity, the significance is marginal ($F(1.544,6.174)=3.583$, $p=.098$, $\eta^2=0.112$).

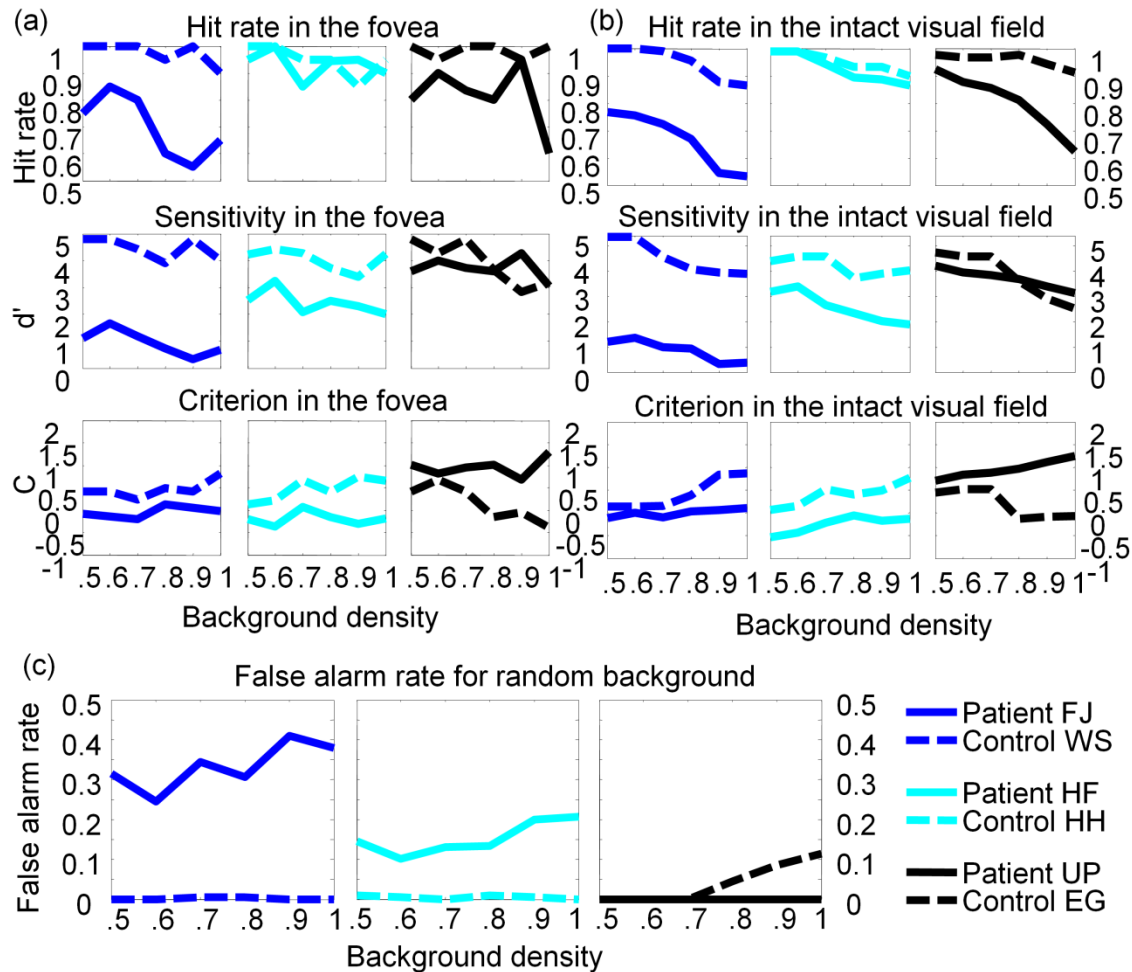


Figure 2. (a) Target (square) presented at 0° (centre). Hit rate, sensitivity measure d' and criterion C for each pair of a hemianopic patient (solid line) and their matched control (dashed line), at each of the six background densities. Top row: hit rate; middle row: d' ; bottom row: C . (b) Target (square) presented in the periphery (0° -centred squares excluded). Hit rate, sensitivity measure d' and criterion C for each hemianopic patient (solid line) across his/her intact hemifield at the six background densities; for comparison, performance of the matched controls is shown (dashed line). Top row: hit rate; middle row: d' ; bottom row: C . (c) Hemianopic patients' false alarm rate (square "detection") when the background only was presented, separately for the six background densities; for comparison, performance of the matched controls is shown.

Pathological completion: background only display

Controls revealed hardly any FA or pathological completion, unlike the hemianopia patients, especially the patients FJ and HF with the cortical lesions. Noteworthy, FJ's FA rate was approximately twice that of HF. This tendency increased with increase in the BD. In comparison, the patient with pre-geniculate lesion, UP, did not reveal any pathological completion (Figure 2(c)).

Pathological completion: square fragments

We expected that pathological completion of square fragments would be triggered more frequently by the following stimulus parameters: (1) higher background densities (BD effect); (2) when the fragment edges face the blind hemifield (fragment orientation effect); (3) when the fragment is presented closer to the border of the blind VF (eccentricity effect).

We carried out a repeated-measures ANOVA for FA to the left- and right-oriented fragments across the entire intact VF. FA rates were averaged across the three meridians for each eccentricity to avoid unbalanced size of presentations of individual fragments. The three within-subjects factors were BD (0.5, 0.6, 0.7, 0.8, 0.9, 1.0), eccentricity (0° , $\pm 5^\circ$, $\pm 10^\circ$, $\pm 15^\circ$) and orientation (binary, i.e., whether the fragment was oriented to the blind hemifield or not); the between-subjects factor was group (patients vs. controls). We found a significant interaction effect for eccentricity and orientation ($F(3,12)=12.357$, $p<.001$, $\eta^2=0.488$). Also significant was the interaction between eccentricity, orientation and group ($F(3,12)=8.987$, $p=.002$, $\eta^2=0.355$; Figure 3(c)). None of the other effects was significant. We found no evidence for the BD effect (1), i.e., increase of FAs for higher BDs, as is indicated by Figure 3(a). Neither was there evidence for the eccentricity effect as such (2), i.e., an increase of FAs when fragments were presented closer to the blind hemifield (Figure 3(b)). The main effect of group (3) was not significant, although we see a definite difference in FA rate between the patient and the control in the FJ–WS pair and HF–HH pair, but not in the UP–EG pair. Patients revealed more FAs when the fragments are close to and oriented towards the blind hemifield (Figure 3(c)). Notably, the orientation effect was reversed for the outermost eccentricity: closer to the fovea, FAs were triggered by the fragments, whose edges faced the blind hemifield; in comparison, when presented in the far periphery, more frequently “completed” were the fragments with the edges oriented away from the blind hemifield. As expected, the orientation of the fragments did not play any role in controls.

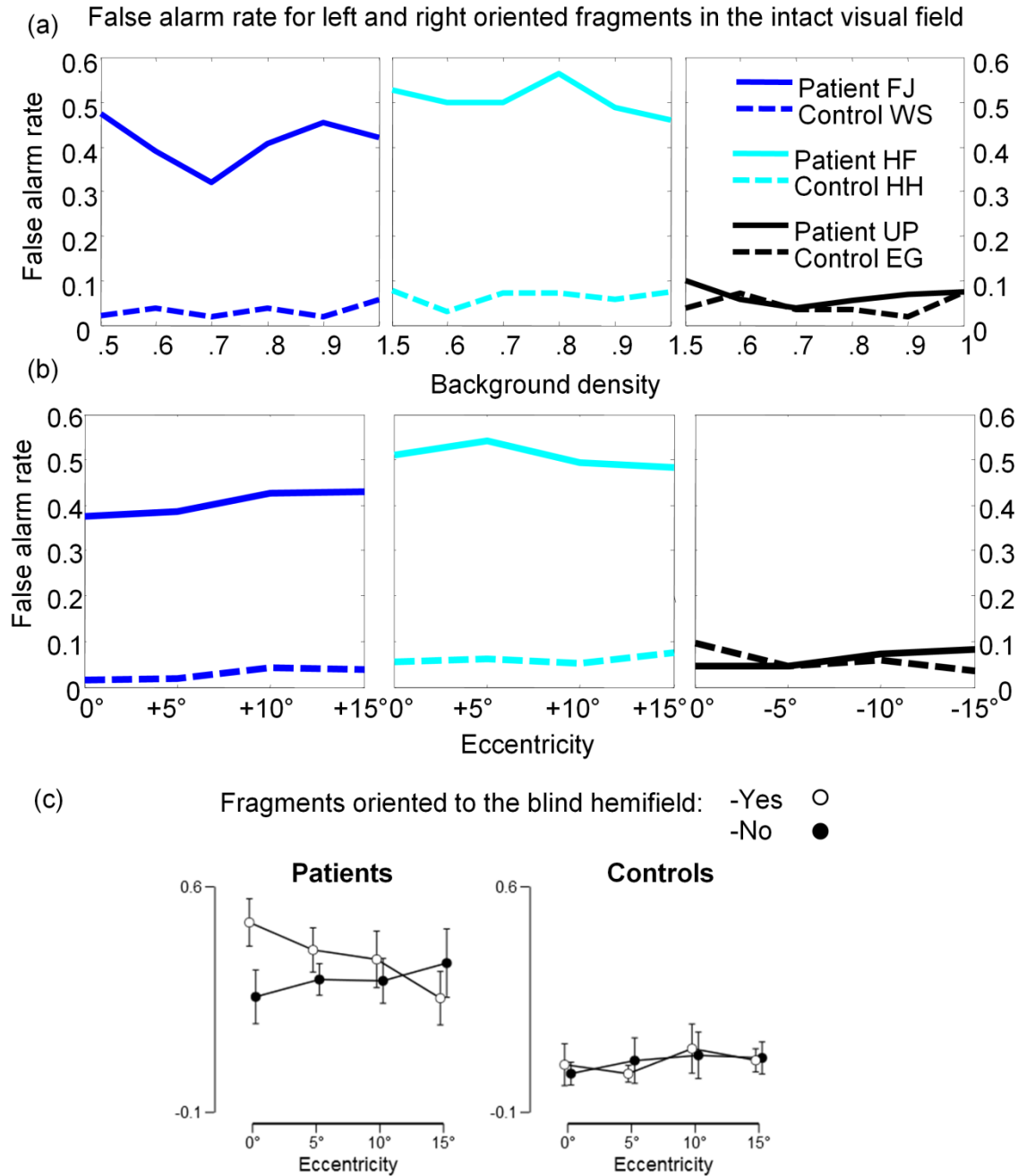


Figure 3. (a) Hemianopic patients' false alarm rate ("detection" of a square when presented with square fragments) for left- and right-oriented fragments at the six background densities; for comparison, performance of the matched controls is shown. (b) False alarm rate for the left- and right-oriented square fragments at the four eccentricities (x-axis indicates eccentricity regardless of its sign). (c) False alarm rate as a function of the fragment orientation in relation to each patient's blind hemifield. The interaction is driven by the patients' performance. As expected, fragment orientation does not play a role for controls.

Figure 4(a) shows results for the fragment “completion” in terms of the COI (see Data analysis), for each patient, across the 19 eccentricities in the entire VF and the six BDs. The COI is colour-coded, with warm colours indicating more frequent FAs for right-oriented fragments and cool colours more frequent FAs for left-oriented fragments. Green colour indicates no difference in the FA rate between the two fragment orientations. We observe idiosyncratic, although above chance level, instances of “completion” of fragments presented in the blind hemifield.

The COI for the fragments presented in the fovea (0°) was significantly different from zero (one-sample t -test) for patients HF ($t(5)=-2.88$, $p=.034$) and UP ($t(5)=4.63$, $p=.006$) but not for patient FJ ($t(5)=-1.59$, $p=.173$). However, for all three patients, the direction of the effect follows the hypothesis (2), as indicated by negative t -values for patient FJ and HF (negative COI) and positive t -value for patient UP (positive COI). In other words, patients FJ and HF “completed” more frequently left-oriented fragments, i.e., with edges facing their left blind hemifield; conversely, patient UP more often “completed” right-oriented fragments, with edges facing her right blind hemifield. Noteworthy, the COI is reversed for the outermost eccentricity ($\pm 15^\circ$), but the effect is not significant (FJ: $t(17)=0.60$, $p=.55$, HF: $t(17)=1.62$, $p=.12$, UP: $t(17)=-1.52$, $p=.15$). Neither was the effect significant for any of the controls; however, two controls showed the tendency in the same direction as their matched patients (HH: $t(17)=0.53$, $p=.60$; EG: $t(17)=-0.444$, $p=.66$), whereas for WS the tendency was in the opposite direction: $t(17)=-1.46$, $p=.16$.

Figure 4(b) visualizes the COIs, pooled over all six BDs, for three VF parts: the blind hemifield (blank, omitted), fovea (0°) and, beyond it, the entire intact hemifield. In schematic representation of the latter, vertical bars colour-code the three eccentricities ($\pm 5^\circ$, $\pm 10^\circ$, $\pm 15^\circ$). It is apparent that patients manifested pathological completion at 0° (centre), when the fragment ends faced the border of the blind hemifield, as colour-coded by central box in Figure 3(a). This tendency, i.e., “completion” of fragments facing the blind hemifield, is also similar for the parafoveal location ($\pm 5^\circ$). Beyond it, at $\pm 10^\circ$, the COI is close to zero, i.e., comparable for both fragment orientations (except for patient FJ, whose performance at $\pm 10^\circ$ is comparable to that in the fovea). Finally, at $\pm 15^\circ$, the tendency changes to the opposite, with more frequent “completion” of fragments with edges facing away from the blind hemifield. Thus, this outcome is in accordance with our hypothesis (2), on the fragment orientation effect. (The COI data for the controls are shown in the Supplemental data Figure S2. For further details, see also Supplemental data Table S2.) We found no evidence that would confirm hypotheses (1) or (3).

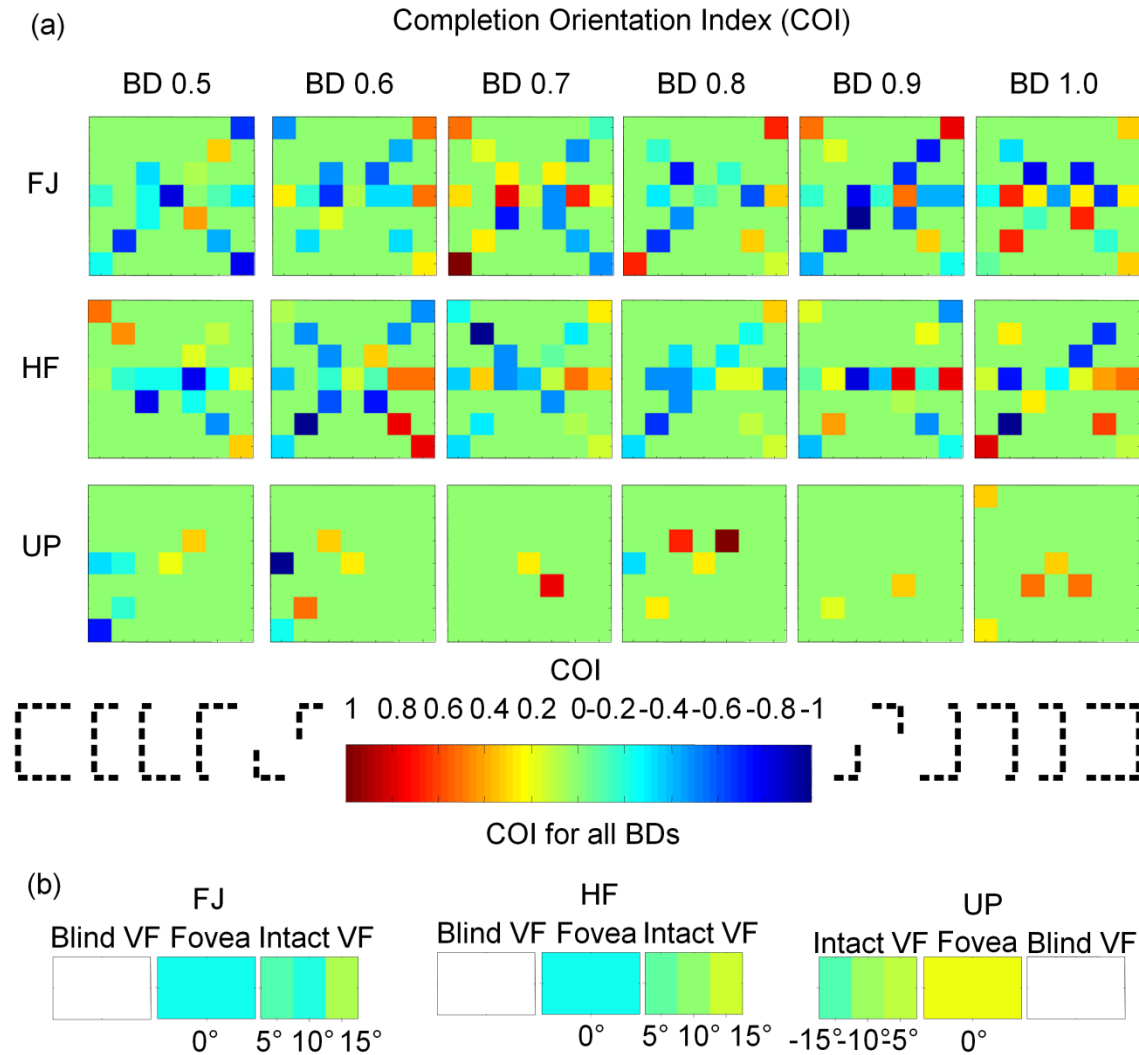


Figure 4. (a) Proportion of incorrect square “detection” by hemianopic patients in the trials with square fragments across the entire visual field. Top row: patient FJ; middle row: patient HF; bottom row: patient UP. Small coloured squares indicate the “Completion Orientation Index” (COI), the difference between the FA rate for right- and left-oriented fragments, at each of the 19 specified locations of the fragment centre. The background density increases from left to right (BD=0.5 through BD=1.0). Colour-code: warm colours: FA greater for right-oriented fragments; cool colours: FA greater for left-oriented fragments. (b) Summary of the top panel. The COI averaged over all BDs in the fovea (0°, centre) and, beyond it, across the intact hemifield, for the three eccentricity locations: 5°, 10° and 15° (right VF) for patients FJ and HF; -5°, -10° and -15° (left VF) for patient UP. The blind hemifield is represented by a white rectangle.

Reaction times

We averaged RTs over all response types for each patient and control. Using repeated-measures ANOVA, we obtained a large main effect of BD ($F(5,20)=8.359$, $p<.001$, $\eta^2=0.568$), no main effect

of group ($F(1,4)=0.003$, $p=.957$, $\eta^2=0.001$) and a marginally significant interaction effect of BD and the group ($F(5,20)=2.370$, $p=.076$, $\eta^2=0.161$). RTs were becoming longer with BD increase. In addition, we explored RTs for the four types of responses – correct square detection (hits), square misses, correct rejection, FA to non-square stimuli – averaged over all BDs, while discounting the BD effect. Figure 5 shows mean RTs of the four response types for each patient, separately for the fovea and periphery of the intact hemifield; for controls, mean RTs are presented for the hemifield analogous to their patient match. In general, patient FJ had longest RTs, followed by patient HF, while patient UP revealed RTs shorter than those of her control match.

The lesion location upstream the visual system (cortical vs. pre-geniculate) appears to play a role for response speed (RTs): the two patients with cortical lesions have longer RTs compared to their matched controls; this is, however, not the case for patient UP. Furthermore, the difference in RTs between the two patients with cortical lesions can be explained by an incomplete hemianopia (residual vision) in patient HF, compared to patient FJ, since it was shown that RTs in the intact hemifield are proportional to the size of the scotoma (Bola et al., 2013b).

In trials with random background display, patient UP was particularly fast for correctly rejecting non-square stimuli (Figure 6(a)). Further, in trials containing a square, we found that eccentricity did not have a strong effect on RTs for correct square detection (Figure 6(b)). Note though that patient FJ's RTs for correctly detected squares increase with the eccentricity. In comparison, RTs of patients HF and UP decrease with eccentricity.

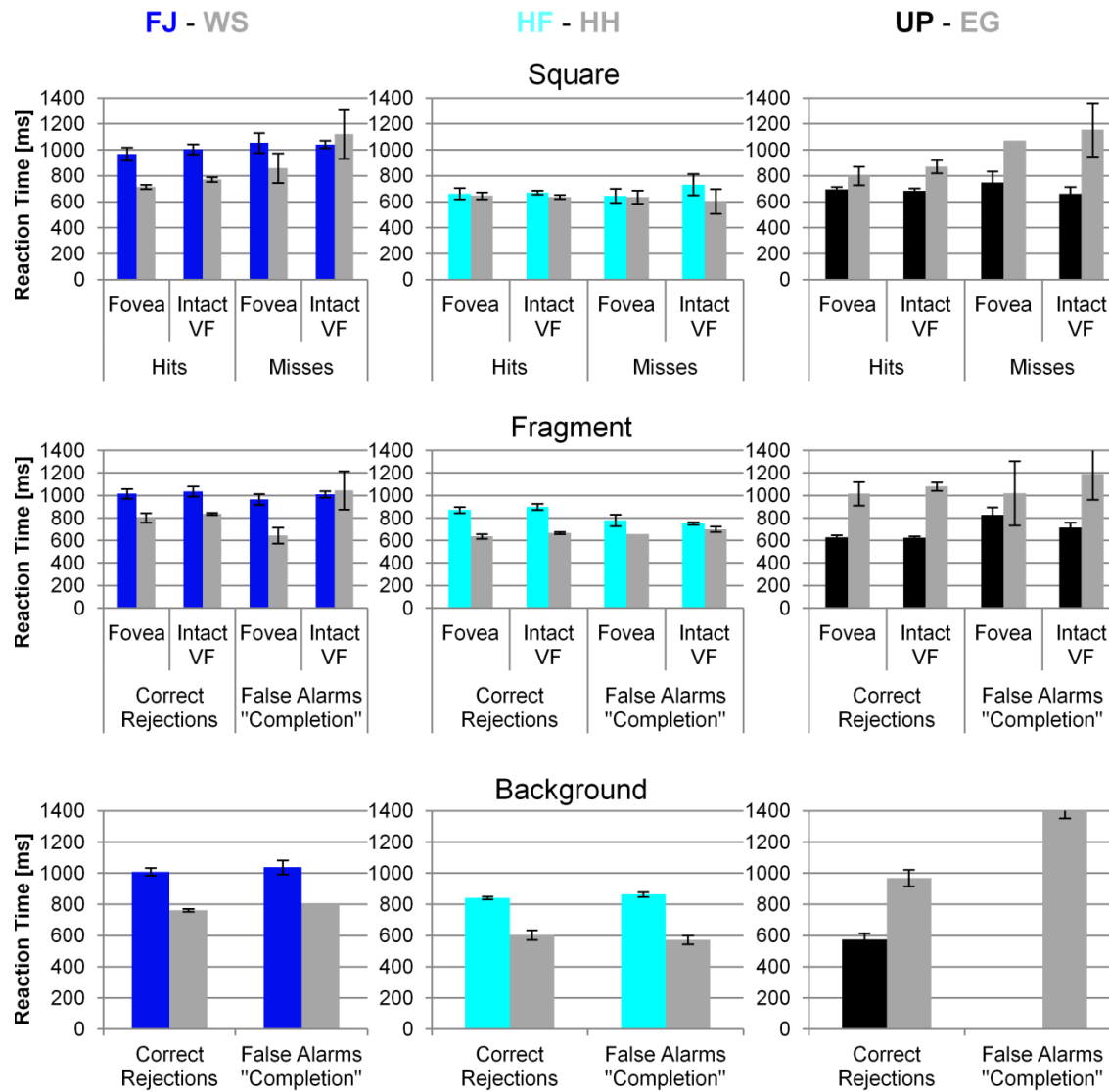


Figure 5. Mean RTs for patients and controls averaged across all BDs. Patients' data are plotted in their corresponding colour: blue FJ (left), cyan HF (middle), and black UP (right); data for matched controls are indicated in grey. First row: hits and misses for square stimuli. Second row: correct rejections and false alarms ("completion") for fragment stimuli. Third row: correct rejections and false alarms for background only display. Two sets of data are presented – for stimuli presented in the fovea and, beyond it, the entire intact VF.

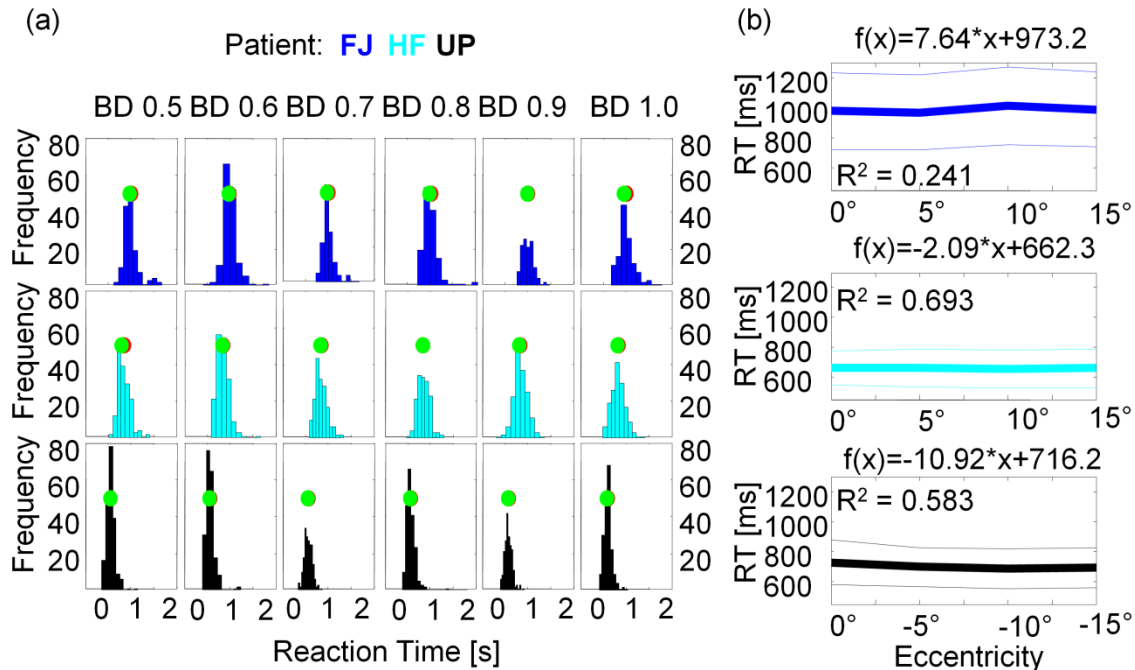


Figure 6. (a) Histograms of RTs for patients' correct rejection in the background only condition for each of the six BDs. Median RT is indicated by the green dot and mean RT by the red dot (mostly hidden). Top row: patient FJ; middle row: patient HF; bottom row: patient UP. (b) Mean RTs of patients' correct square detection in the intact hemifield as a function of the figure eccentricity. Top: patient FJ; middle: patient HF; bottom: patient UP. Thick solid line represents mean RTs, thin lines represent 1 standard deviation above and below the mean. Linear fitting statistics is shown for each plot.

Discussion

Hemianopic patients revealed deficits not only in the blind VF but also in the *intact* ipsilateral VF, deficits manifested as erroneous “completion” of incomplete figures or “detection” of a non-present figure. This “hyperfunction” in the intact VF may be attributed to lack of input of neural signals from the contralateral blind field. This is in accord with a line of reasoning that holds that “the lesion causes more wide-spread abnormalities ... the visual information within the damaged hemisphere to be reduced and delayed, and this has consequences for the interhemispheric functional connectivity and down-stream visual processing” (Geuzebroek & van den Berg, 2017, p. 161). This view is supported by significantly reduced synchronization in gamma-band (Schadow et al., 2009), electrophysiological “signature” of the contour integration and recognition of Gestalts.

Specifically with regards to the “pathological completion”, there are two explanatory schemes, both implying the involvement of *implicit inferences* interwoven into visual perception hypotheses. First, as was assumed by Poppelreuter (1917/1990, p. 13), “completion” is produced by a “totalizing Gestalt conception” (*totalisierende Gestaltauffassung*), implying filling-in of missing

parts in familiar figures. Poppelreuter attributed this type of completion to the function of apperception, i.e., activation of shape representations, which invokes the Gestalt concepts of “closure”, “continuation” and “symmetry”, and considered it as *imaginative* in nature.

Poppelreuter’s interpretation (imaginative completion) is compatible with Warrington’s (1965) findings for simple and “good” geometric figures; however, it fails to account for instances of absence of “completion”. Importantly, it was shown that pathological completion is closely associated with lesions involving the parietal area and related to patient’s poor insight into their visual defect (Mattingley & Walker, 2003; Sergent, 1988; Warrington, 1962, 1965).

Alternatively, “pathological completion” was argued to result from ignoring the missing part of a figure, rather than active filling-in, the explanation that alludes to the well-known visuo-attentional deficits in hemianopia patients (Marcel, 1998; Walker & Mattingley, 1997; Weiskrantz, Barbur, & Sahraie, 1995). The role of visual inattention and (lack of) awareness is underscored by the fact that not all hemianopia patients manifest pathological completion: its relative frequency amounted to 40% (Pollack et al., 1957) or 55% (Warrington, 1962). Notably, “completion” was found to be reduced or disappeared when hemianopia patients’ attention was directed to the error and critical attitude was induced (Fuchs, 1921/1938; Gassel & Williams, 1963).

Adherents of both views agree though that fragmented figures are often completed to full figures, increasing the FA rate. This view is supported in a recent study of Geuzebroek and van den Berg (2017) who conclude that response pattern of hemianopia patients is affected by a strong tendency to guess.

With regards to the BD, we observed decrease in patients’ performance with increasing BDs, a result in agreement with previous findings (Kovács et al., 2000, for amblyopia; Paramei & Sabel, 2008, for hemianopia; Roudaia, Bennett, & Sekuler, 2013, for healthy elderly). In the present study, correct figure detection (hit rate) decreased in patients more distinctly compared to controls when the number of distracters increased, suggesting a deficient contextual processing in the intact VF, although the interaction does not hold when correcting for sphericity violation. We are tempted to conjecture that the difference in the hit rate of patients and matched controls is greater for $BD=1.0$, “noisy” background, than $BD=0.5$, implying that patients’ performance is stronger impaired at high BDs than that of controls. This holds true for both foveal, parafoveal and peripheral vision for patients with both cortical and optic-tract lesions but to a lesser degree for the latter. These results are mainly explained by a decrease in sensitivity rather than a change of criterion, except for patient UP, who showed also a shift of the criterion along with a decrease in sensitivity (Figures 2 (a and b)). For the background only condition, the FA rate increased, too, with BD (Figure 2(c)). Both kinds of performance deficits indicate that contextual processing is strongly affected in the intact field.

We can only speculate about the underlying mechanisms. In terms of sensitivity d' , in the fovea patients’ performance is deteriorated compared to their matched controls, but it does not change with the BD. In contrast, in the intact VF, the patients’ performance strongly deteriorates the more distracters are present, with the decline pronounced much more in the patients than controls. This is reflected by the interaction for group and BD.

These findings are reminiscent of the characteristics of crowding performance, which usually is very little affected in the fovea but strongly declines for peripheral vision (Levi, 2008). The main effect may reflect unspecific processing deficits induced by the lesion in hemianopia patients. One explanation is that processing in cluttered displays in the right VFs depends on processing in the left field and vice versa. Sayim, Greenwood, and Cavanagh (2014) found that strong crowding of a letter (E) in the right VF can be improved when the same letter is presented at the corresponding position in the left VF. Similar processes may have played a role for the display used here. However, as mentioned, these considerations remain speculation at the moment.

Contour detection is limited by the relative spacing between the contour and the background elements (Braun, 1999). A greater proximity of distracters to each other increases the likelihood of a chain of distracters grouping together to form false-positive contours (Gilad, Meirovithz, & Slovin, 2013; V1, monkeys). In the latter study, contour integration in a “noisy” background was reflected in a “surround suppression” phenomena at a rather late stage (140 ms after stimulus onset) of visual processing. This can be attributed either to (1) feedforward influences implying local interactions (thalamic input) or to (2) feedback influences (top-down control) related to perceptual processes. In our case, patients do not receive the thalamic input since the cortex is damaged, which leaves only top-down control deficits. The higher rate of FAs probably indicates deficit of the “surround suppression”, meaning a decrease in the top-down suppression (i.e., inhibition) of the responses to the background distracters.

First, we expected a higher rate of pathological completion at higher BDs. We found no evidence for such effect. Second, we expected more pathological completion in the fovea when the fragment edges were oriented to and abutting the border of the blind VF (Figure 4) since in this case the patient may fill-in the missing parts in the same way as healthy individuals fill-in information at the blind spot. Patient FJ and HF make more FAs for right-oriented fragments, i.e., facing their right blind hemifield, while patient UP makes more FAs for left-oriented fragments, i.e., facing her left blind hemifield. Surprisingly, we observed the opposite tendency for the most peripheral locations, although the effect was not significant. Possibly, the fragment edges are poorly detectable at the VF periphery. Third, we did not find any evidence for FA rate reduction as a function of eccentricity.

It was argued that pathological completion does not occur when incomplete stimuli are presented elsewhere in the intact hemifield (McCarthy et al., 2006; Weil et al., 2009). At odds with this proposition is our finding that pathological completion occurred across the entire intact VF. Note though that the former conclusion was inferred from the studies with incomplete figures made of solid contours, with low-spatial frequency stimuli displayed on a homogeneous background under relatively high contrast conditions.

As mentioned in the introductory section, the “completion” phenomenon was observed to be related to lesions extending to parietal lobe (Warrington, 1962, 1965). Indeed, we found that the patients HF and FJ, with lesions extending to temporo-parietal area, have higher rate of FAs compared to the patient UP who does not, prompting that “pathological completion” appears to be more likely associated with lesions of cortical rather than geniculostriate origin. However, the

low number of patients studied here and, in particular, just one patient with subcortical lesion in the sample, requires caution in claiming the effect of lesion location.

Further, both FJ and HF suffer from right cortical lesion. Brain asymmetries were shown to play a role in the heterogeneity of the functional deficits. In his work, Humphreys (1996) reports that right brain injury is often associated with deficits in perceptual organization such as the Gestalt principle of closure. In particular, compared to left brain damage patients, patients with lesions involving the right occipital lobe have impaired naming performance of fragmented figure leading to stronger deficits (see also Warrington & James, 1967). In the present study, with just three cases, the evidence is insufficient to make any claims on lesion lateralization-related deficits.

Finally, we found that hemianopia patients had longer reaction times than controls, in accordance with previous studies. The two patients with cortical lesions, FJ and HF, were slower than their matched controls. Patient UP was, surprisingly, even faster than her matched control (Figures 5 and 6(a); Supplemental data Figure S3 for each VF location; Table S1 for each BD). This finding indicates that the lesion location upstream the visual system plays a role in response speed. We found little evidence that RTs increase the more peripherally the targets were presented. This is in agreement with findings of Bola et al. (2013b) who showed that reaction times were longer when the stimuli were presented closer to the scotoma, but is at odds with the findings of Poggel et al. (2011), for a light detection task in which RTs increase slightly and monotonously toward the periphery of the visual field. The latter was true only for one patient, FJ, whose RTs increased with eccentricity. But the opposite was true for the two other patients: RTs decreased slightly with eccentricity for patient HF and strongly for patient UP (Figure 6(b)) supporting evidence for a local (retinotopic) effect of the scotoma on the detection task performance. Overall, RTs indicated that hemianopia patients with cortical lesions are in general slower compared to healthy controls. Notably, responses of FJ, patient with occipito-parietal lesion, were the longest, indicating the significance of the lesion location upstream of the visual pathway. HF's RTs were shorter than FJ's, the difference that may be attributed either to his lesion affecting occipital cortex and/or explained by his incomplete hemianopia (residual vision), since it was shown that RTs in the intact hemifield are proportional to the size of the scotoma (Bola et al., 2013b). Since in the case of patient HF these two factors are confounded, currently we cannot definitely conclude about the role of the lesion location in the visual system, and further investigation is necessary to disentangle the factors related to RT differences.

Limitations

There are several limitations to this study. The sample size with just three patients was small. Lack of recording of eye movements is another limitation, since, in general, hemianopic patients are reported to have an instable central fixation and/or a tendency to eccentric fixation (Gassel & Williams, 1963; Trauzettel-Klosinski & Reinhard, 1998). If our patients were unable to maintain accurate fixation, this might explain the above-chance rate of pathological completion obtained for their blind hemifield. Alternatively, it is also possible that patients have just "completed" the random background visible in the intact hemifield. Finally, we are aware that in our study the number of trials with the square fragment stimuli per location in the VF was rather low and thus is the statistical power. In spite of these limitations, our results are consistent with the previous

reports on Gestalt deficits in the “intact” field of hemianopia patients and on the role of contextual interaction.

Conclusions

Hemianopia patients reveal deficits of figure integration in their intact hemifield whereby they may either miss detecting a figure (square) embedded in a “noisy” background or report seeing the figure when none or its fragments are presented, revealing a pronounced tendency to guess. The orientation of the square fragments was found to play the role: for foveally presented stimuli, FA increased when fragment edges faced the patient’s blind hemifield; conversely, for outermost periphery of the intact VF, FA were more frequent for fragments oriented away from the blind hemifield. Pathological completion occurred more frequently for higher BDs (in particular, $BD=0.9$ and $BD=1.0$). The “noisy background” effect indicates that a “crowded” context engenders contour integration deficits in the “intact” VF of hemianopia patients, which may explain why hemianopia patients report being uncomfortable in crowded places in everyday life.

Acknowledgements

The authors wish to thank U. Bunzenthal for excellent assistance in recruiting subjects. We are grateful to C. Altmann for making available his stimulus program, to B. Herwig for developing the software for stimulus generation, to U. Polat and L. Spillmann for insightful comments on the experiment design. We thank the subjects of this study for their time, understanding and collaborative spirit. Results were partly presented at the 38th European Conference on Visual Perception, 23–27 August 2015, Liverpool, UK. We are grateful to two anonymous reviewers whose detailed and constructive comments to an earlier version of the manuscript were helpful for improving the paper.

Disclosure statement

No potential conflict of interest was reported by the authors

Funding

This work was supported by the Swiss National Science Foundation (SNF) Grant # 51NF40-158776, the National Centre of Competence in Research (NCCR) “SYNAPSY–The Synaptic Basis of Mental Diseases”, to OF and MHH from the École Polytechnique Fédérale de Lausanne, Switzerland.

References

- Bender, M.B. & Teuber, H.-L. (1946). Phenomena of fluctuation, extinction and completion in visual perception. *Archives of Neurology and Psychiatry*, 15, 627-658.
- Bola, M., Gall, C., & Sabel, B.A. (2013a). "Sightblind": Perceptual deficits in the "intact" visual field. *Frontiers in Neurology*, 4:80. doi: 10.3389/fneur.2013.00080
- Bola, M., Gall, C., & Sabel, B.A. (2013b). The second face of blindness: Processing speed deficits in the intact visual field after pre- and post-chiasmatic lesions. *PLoS ONE*, 8(5): e63700. <http://doi.org/10.1371/journal.pone.0063700>
- Braun, J. (1999). On the detection of salient contours. *Spatial Vision*, 12, 211-225.
- Cavézian, C., Perez, C., Peyrin, C., Gaudry, I., Obadia, M., Gout, M., & Chokron, S. (2015). Hemisphere-dependent ipsilesional deficits in hemianopia: Sightblindness in the "intact" visual field. *Cortex*, 69, 166-174.
- Cavézian, C., Gaudry, I., Perez, C., Coubard, O., Doucet, G., Peyrin, C., Marendaz, C., Obadia, M., Gout, M., & Chokron, S. (2010). Specific impairments in visual processing following lesion side in hemianopic patients. *Cortex*, 46, 1123-1131.
- Chokron, S., Perez, C., & Peyrin, C. (2016). Behavioral consequences and cortical reorganization in homonymous hemianopia. *Frontiers in Systems Neuroscience*, 10:57. doi: [10.3389/fnsys.2016.00057](https://doi.org/10.3389/fnsys.2016.00057)
- Field, D.J., Hayes, A., & Hess, R.F. (1993). Contour integration by the human visual system: Evidence for a local "association field". *Vision Research*, 33, 173-193.
- Fuchs, W. (1920). Untersuchung über das Sehen der Hemianopiker und Hemiamblyopiker. – I. Verlagerungserscheinungen. *Zeitschrift für Psychologie*, 84, 64-169.
- Fuchs, W. (1921/1938). Completion phenomena in hemianopic vision. Translated by W.D. Ellis. In *A source book of Gestalt Psychology* (pp. 344-356). London: Kegan Paul.
- Gassel, M. M. & Williams, D. (1963). Visual function in patients with homonymous hemianopia—III. The completion phenomenon: Insight and attitude to the defect and visual function efficiency. *Brain*, 86, 229-260.
- Geuzebroek, A.C., & van den Berg, A.V. (2017). Impaired visual competition in patients with homonymous visual field defects. *Neuropsychologia*, 97, 152-162.
- Giersch, A., Humphreys, G.W., Boucart, M., & Kovács, I. (2000). The computation of occluded contours in visual agnosia: Evidence for early computation prior to shape binding and figure-ground coding. *Cognitive Neuropsychology*, 17, 731-759.
- Gilad, A., Meirovitz, E., & Slovin, H. (2013). Population responses to contour integration: Early encoding of discrete elements and late perceptual grouping. *Neuron*, 78, 389-402.
- Gilchrist, I.D., Humphreys, G.W., & Riddoch, M.J. (1996). Grouping and extinction: Evidence for low-level modulation of visual selection. *Cognitive Neuropsychology*, 13, 1223-1249.

- Han, S., & Humphreys, G.W. (2007). The fronto-parietal network and top-down modulation of perceptual grouping. *Neurocase*, *13*, 278-289.
- Hautus, M.J. (1995). Corrections for extreme proportions and their biasing effects on estimated values of d' . *Behavior Research Methods, Instruments, & Computers*, *27*, 46-51.
- Hess, R.F., & Pointer, J.S. (1989). Spatial and temporal contrast sensitivity in hemianopia: A comparative study of the sighted and blind hemispheres. *Brain*, *112*, 871-894.
- Humphreys, G.W. (1996). Processing fragmented forms and strategic control of orienting in visual neglect. *Cognitive Neuropsychology*, *13*, 177-204.
- Humphreys, G.W. (2001). A multi-stage account of binding in vision: Neuropsychological evidence. *Visual Cognition*, *8*, 381-410.
- Humphreys, G.W. (2003). Conscious visual representations built from multiple binding processes: Evidence from neuropsychology. *Progress in Brain Research*, *142*, 243-255.
- Kovács, I., & Julesz, B. (1993). A closed curve is much more than an incomplete one: Effect of closure in figure-ground segmentation. *Proceedings of the National Academy of Sciences of the USA*, *90*, 7495-7497.
- Kovács, I., Polat, U., Pennefather, P.M., Chandna, A., & Norcia, A.N. (2000). A new test of contour integration deficits in patients with a history of disrupted binocular experience during visual development. *Visual Research*, *40*, 1775-1783.
- Levi, D.M. (2008). Crowding—An essential bottleneck for object recognition: A mini-review. *Vision Research*, *48*, 635-654.
- Marcel, A.J. (1998). Blindsight and shape perception: Deficit of visual consciousness or of visual function? *Brain*, *191*, 1565-1588.
- Mattingley, J.B., & Walker, R. (2003). The blind leading the mind: Pathological visual completion in hemianopia and spatial neglect. In L. Pessoa, P. de Weerd (Eds.), *Filling-in: From perceptual completion to cortical reorganization* (Ch. 11, pp. 207-227). Oxford: Oxford University Press.
- McCarthy, R., James-Galton, M., & Plant, G.T. (2006). Form completion across hemianopic boundary: Behindsight? *Neuropsychologia*, *44*, 1269-1281.
- Paramei, G.V., & Sabel, B.A. (2008). Contour-integration deficits on the intact side of the visual field in hemianopia patients. *Behavioural Brain Research*, *188*, 109-124.
<http://doi.org/10.1016/j.bbr.2007.10.025>
- Poggel, D.A., Treutwein, B., & Strasburger, H. (2011). Time will tell: Deficits of the temporal information processing in patients with visual field loss. *Brain Research*, *1368*, 196-207.
- Polat, U., & Bonneh, Y. (2000). Collinear interactions and contour integration. *Spatial Vision*, *13*, 393-401.
- Pollack, M., Battersby, W.S., & Bender, M.B. (1957). Tachistoscopic identification of contour in patients with brain damage. *Journal of Comparative Physiological Psychology*, *50*, 220-227.

- Poppelreuter, W. (1917/1990). *Disturbances of lower and higher visual capacities caused by occipital damage: With special reference to the psychopathological, pedagogical, industrial, and social implications*. Translated by J. Zihl, L. Weiskrantz. Oxford: Clarendon Press.
- Rizzo, M., & Robin, R.A. (1996). Bilateral effects of unilateral visula cortex lesions in human. *Brain*, *119*, 951-963.
- Roudaia, E., Bennett, P.J., & Sekuler, A.B. (2013). Contour integration and aging: The effects of element spacing, orientation alignment and stimulus duration. *Frontiers in Psychology*, *4*:356. doi: 10.3389/fpsyg.2013.00356
- Sayim, B., Greenwood, J.A., & Cavanagh, P. (2014). Foveal target repetitions reduce crowding. *Journal of Vision*, *14*(6):4. doi:10.1167/14.6.4
- Schadow, J., Dettler, N., Paramei, G.V., Lenz, D., Fründ, I., Sabel, B.A., & Herrmann, C.S. (2009). Impairments of Gestalt perception in the intact hemifield of hemianopic patients are reflected in gamma-band EEG activity. *Neuropsychologia*, *47*, 556-568.
- Sergent, J. (1988). An investigation into visual completion in blind areas of the visual field. *Brain*, *111*, 347-373.
- Totjussen, T. (1978). Visual processing in cortically blind hemifields. *Neuropsychologia*, *16*, 15-21.
- Trauzettel-Klosinski, S., & Reinhard, J. (1998). The vertical field border in hemianopia and its significance for fixation and reading. *Investigative Ophthalmology & Visual Science*, *39*, 2177-2186.
- Vancleef, K., Wagemans, J., & Humphreys, G.W. (2013). Impaired texture segregation but spared contour integration following damage to right posterior parietal cortex. *Experimental Brain Research*, *230*, 41-57.
- Walker, R., & Mattingley, J.B. (1997). Ghosts in the machine? Pathological visual completion phenomena in the damaged brain. *Neurocase*, *3*, 313-335. <http://doi.org/10.1080/13554799708411972>
- Warrington, E.K. (1962). The completion of visual forms across hemianopic field defects. *Journal of Neurology, Neurosurgery & Psychiatry*, *25*, 208-217.
- Warrington, E.K. (1965). The effect of stimulus configuration on the incidence of the completion phenomenon. *British Journal of Psychology*, *56*, 447-454.
- Warrington, E.K., & James, M. (1967). Disorders of visual perception in patients with localised cerebral lesions. *Neuropsychologia*, *5*, 253-266.
- Weil, R. S., Plant, G.T., James-Galton, M., & Rees, G. (2009). Neural correlates of hemianopic completion across the vertical meridian. *Neuropsychologia*, *44*, 457-464.
- Weiskrantz, L. Barbur, J.L., & Sahraie, A. (1995). Parameters affecting conscious versus unconscious visual discrimination with damage to the visual cortex (V1). *Proceedings of the National Academy of Sciences of the USA*, *92*, 6122-6126.

Supplemental data

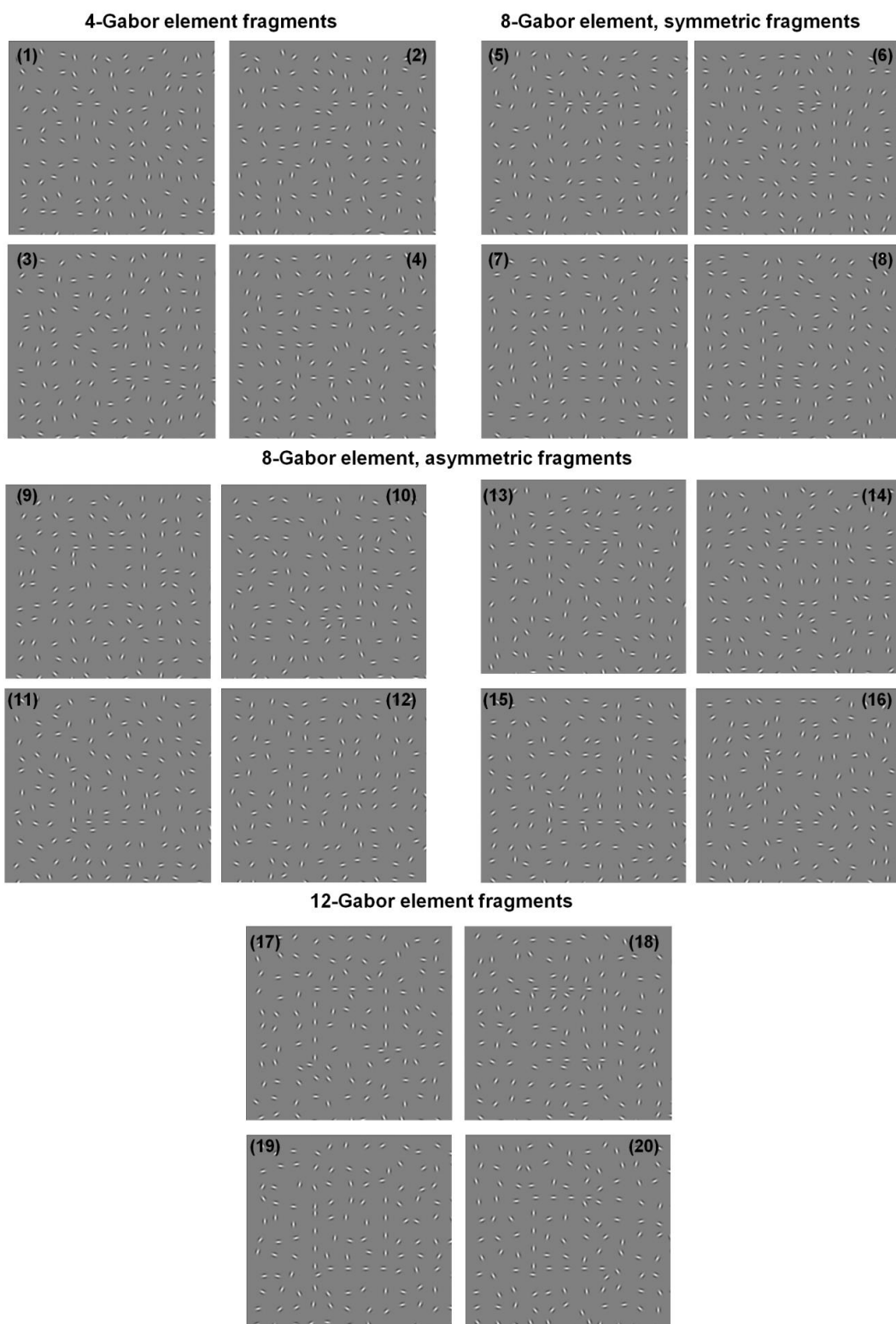


Figure S1. Square fragments ($N=20$). Examples with $BD=1.0$.

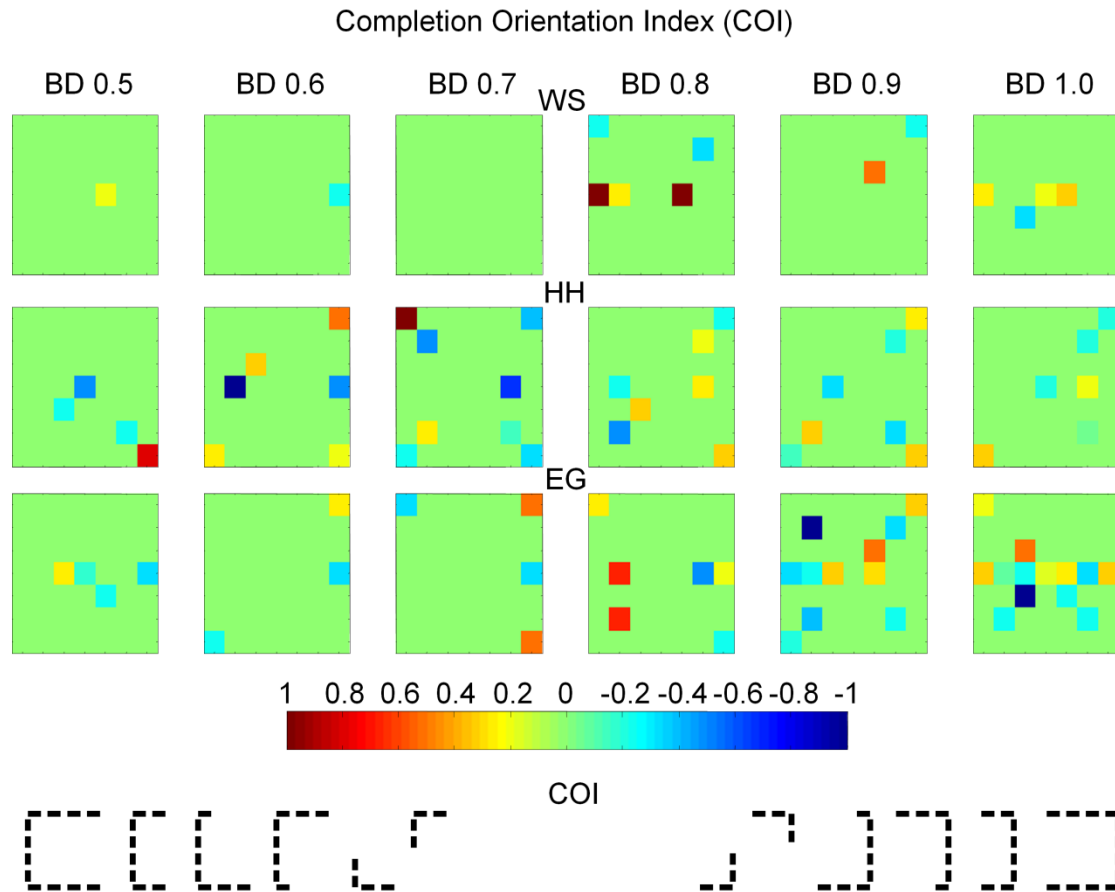


Figure S2. Proportion of incorrect square “detection” for healthy controls in the trials with square fragments, across the entire visual field. Top row: WS (match of patient FJ); middle row: HH (match of patient HF); bottom row: EG (match of patient UP). Small coloured rectangles indicate the “Completion Orientation Index” (COI), the difference between FA rate of right- and left-oriented fragments, at each of the 19 specified locations of the fragment centre. The background density increases from left to right (BD=0.5 through BD=1.0). Colour-code: warm colours: FA greater for right-oriented fragments; cool colours: FA greater for left-oriented fragments.

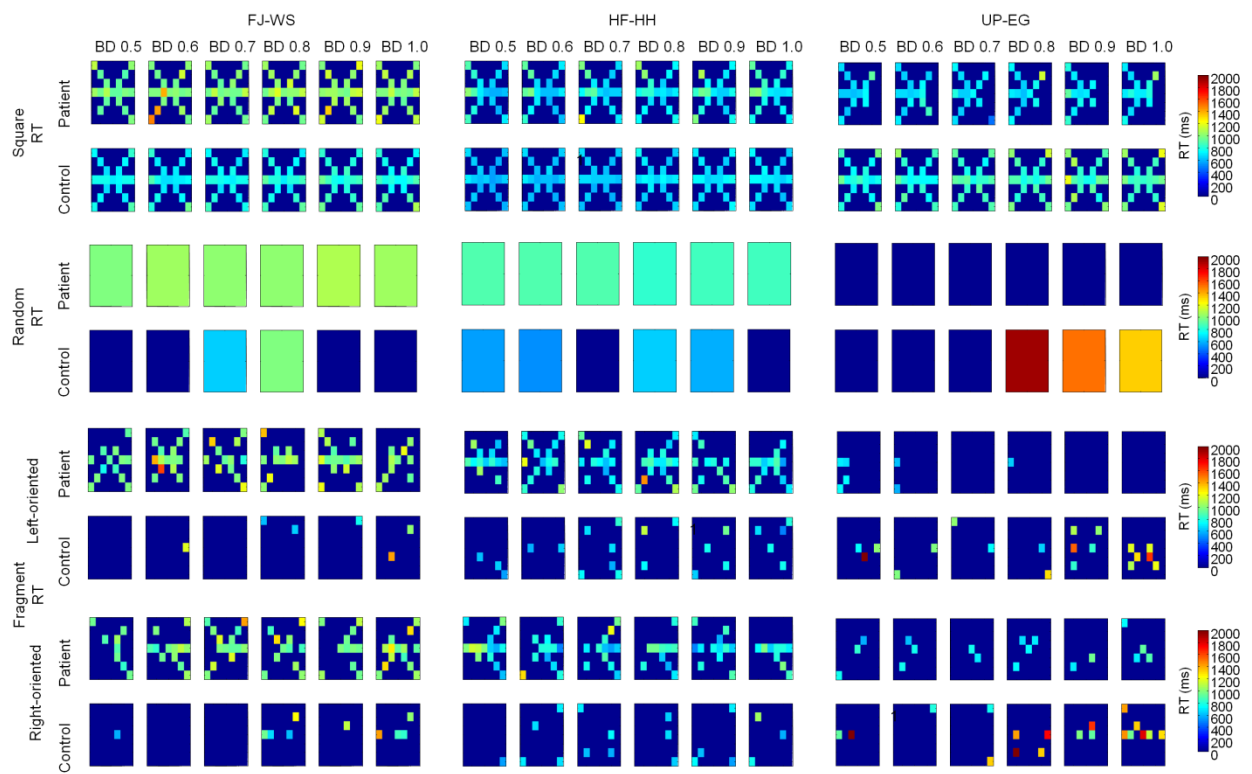


Figure S3. Map of mean reaction times for the three patient-matched control pairs (paired rows in each columns) across the six background densities and for four different stimulus categories (rows). Mean RTs are colour-coded as is indicated by the scale at the right.

			FJ-WS					HF-HH					UP-EG									
			BD 0.5	BD 0.6	BD 0.7	BD 0.8	BD 0.9	BD 1.0	BD 0.5	BD 0.6	BD 0.7	BD 0.8	BD 0.9	BD 1.0	BD 0.5	BD 0.6	BD 0.7	BD 0.8	BD 0.9	BD 1.0		
Square	Patient	Hits	Fovea	mean	933.33	970.71	993.31	977.08	975.82	965.92	609.42	606.50	668.06	663.94	712.11	716.56	632.25	685.44	722.40	732.25	690.47	714.33
			Intact	SD	128.88	185.70	166.42	200.05	81.63	88.99	104.63	58.80	107.81	74.98	182.44	115.16	71.26	68.70	119.74	102.30	79.96	89.58
			VF	mean	951.28	1000.46	974.92	1037.97	1048.59	1014.33	629.33	631.67	660.52	693.28	692.19	716.95	651.24	660.74	680.47	665.53	735.22	707.63
		Misses	Fovea	mean	937.40	935.00	1156.75	1039.25	1141.78	1116.00	601.00	571.00	711.00	491.00	856.00	868.75	826.00	714.33	701.00	661.00	717.25	
			Intact	SD	59.11	202.90	207.57	173.30	294.47	214.74	0.00	65.57	0.00	0.00	120.21	229.38	91.92	41.63	176.64	0.00	128.94	
			VF	mean	984.33	1120.27	1047.64	1052.31	1024.17	1020.55	561.00	741.00	677.00	822.22	798.10	793.67	651.00	638.36	603.31	745.24	689.40	642.18
	Control	Hits	Fovea	mean	716.50	673.00	722.00	708.89	730.00	737.11	632.50	606.00	639.95	637.84	672.76	690.47	850.70	761.00	766.55	836.15	763.16	819.55
			Intact	SD	103.34	98.65	106.42	107.27	138.22	128.11	101.68	51.66	60.08	56.48	108.99	102.93	281.82	101.11	97.38	118.32	130.85	117.73
			VF	mean	752.50	734.30	734.84	781.91	824.54	802.42	583.92	614.93	615.95	659.31	696.02	655.39	790.92	837.00	864.25	872.00	969.57	886.40
		Misses	Fovea	mean	152.38	162.55	131.09	155.01	149.28	183.39	59.60	77.13	78.06	70.85	102.52	82.18	134.65	220.67	171.44	193.89	282.97	182.21
			Intact	SD				411.00	1307.00			581.00	761.00	611.00	591.00		681.00				1462.00	
			VF	mean			1552.00	1164.25	980.64	791.25	551.00	401.00	684.33	649.33	709.33	617.67	1758.00	1101.67	958.00	691.00	1151.80	1264.38
Square Fragments	Patient	Correct Rejections	Fovea	mean	940.11	1080.29	1018.38	894.56	1106.75	1050.73	878.10	944.89	785.00	882.22	891.33	843.44	613.83	636.88	665.44	603.22	642.11	599.95
			Intact	SD	112.46	214.03	111.19	135.75	183.08	181.87	152.93	151.91	103.09	155.17	190.82	138.46	137.01	108.63	140.22	100.03	134.47	90.67
			VF	mean	1011.17	1060.17	996.67	1039.71	1055.09	1053.20	943.03	924.87	904.18	845.97	868.68	905.70	647.79	632.38	608.53	606.01	622.49	634.87
		False Alarms "Completion"	Fovea	mean	179.05	169.06	116.51	155.39	185.63	249.66	199.92	163.20	160.83	158.56	121.84	191.38	138.13	125.66	114.96	132.49	127.09	107.20
			Intact	SD	951.36	947.46	958.29	980.55	1019.83	937.00	747.78	712.91	795.00	804.20	804.71	807.55	856.00	751.00	881.00	741.00	801.00	931.00
			VF	mean	99.68	52.55	37.12	73.68	171.10	81.73	235.05	129.75	88.72	193.92	147.06	189.55	21.21	45.83	183.85	56.57	0.00	0.00
	Control	Correct Rejections	Fovea	mean	953.58	1015.91	1011.06	1027.00	1027.89	1029.49	706.88	751.41	735.98	746.67	789.06	784.33	744.00	653.00	861.00	656.00	691.00	675.29
			Intact	SD	109.23	121.19	128.50	121.69	152.35	187.89	145.79	145.87	140.51	127.12	138.39	119.01	109.65	66.80	0.00	74.50	0.00	83.24
			VF	mean	835.70	788.05	816.84	787.55	766.26	818.24	606.26	643.63	614.00	616.79	692.50	644.53	1027.84	892.70	942.80	1023.45	1121.16	1083.44
		False Alarms "Completion"	Fovea	mean	169.53	116.09	109.55	136.16	128.30	221.46	78.41	105.30	53.22	55.51	95.11	80.39	463.76	207.74	154.33	293.60	256.41	256.02
			Intact	SD	874.49	839.09	841.53	848.35	811.12	811.78	652.01	637.51	660.51	657.60	702.61	689.14	996.91	1011.83	1074.70	1156.20	1110.21	1126.19
			VF	mean	190.93	173.84	186.54	178.77	171.08	165.58	113.88	98.21	101.89	97.32	124.85	113.19	234.18	278.72	301.38	331.94	331.90	277.37
Random Background	Patient	Correct Rejections	Fovea	mean																		
			Intact	SD	744.33	1053.60	1242.00	1238.00	869.60	1121.67	618.00	688.50	709.00	728.50	789.88	665.62	1198.33	936.00	1187.80	1313.93	1236.79	1258.75
			VF	mean	155.35	402.67	452.33	614.98	219.71	262.21	114.99	127.59	103.69	91.46	161.27	130.36	689.20	63.64	357.10	444.52	545.24	211.19
		False Alarms "Completion"	Fovea	mean	1005.47	999.32	1008.24	1030.30	1004.39	1007.96	844.16	847.22	843.53	841.32	836.30	834.02	555.91	569.12	567.55	578.14	580.70	599.36
			Intact	SD	176.90	157.08	145.50	192.21	131.35	184.65	137.63	141.07	140.54	131.75	153.11	154.15	98.39	112.56	87.06	190.48	84.60	94.60
			VF	mean	997.52	1045.92	1022.16	1030.77	1067.84	1061.80	881.96	878.25	875.24	817.75	856.56	874.00						
	Control	Correct Rejections	Fovea	mean	98.02	118.44	127.84	154.73	218.84	189.30	166.43	151.49	169.79	129.30	158.83	170.49						
			Intact	SD	747.46	749.77	757.38	767.14	777.73	774.94	554.79	575.10	593.69	607.67	635.66	656.36	880.21	892.39	957.72	1047.57	1029.86	1006.63
			VF	mean	138.66	162.45	146.11	140.35	139.03	156.79	58.63	76.41	81.91	73.06	127.97	130.75	212.78	218.63	255.25	346.62	321.50	264.04
		False Alarms "Completion"	Fovea	mean			631.00	971.00			551.00	531.00		636.00	571.00					1908.44	1509.35	1340.35
			Intact	SD			0.00	0.00			56.57	0.00		35.36	0.00					660.00	289.44	227.54
			VF	mean																		

Table S1. RT mean and standard deviation (SD) for each patient-matched control pair, each type of stimuli and each BD. Separately presented are data for the fovea and, beyond it, the entire intact hemifield. RT means were computed for hits, misses, correct rejections and false alarms ("completion"). Patients' data are highlighted in light grey. Blank areas indicate that there were no responses on trials corresponding to the set of parameters in question. SD=0 indicates that there was only one trial for the set of parameters in question.

	BD 0.5			BD 0.6			BD 0.7			BD 0.8			BD 0.9			BD 1.0		
FJ	Left	0.00	0.67	0.50	0.00	0.00	0.00	0.00	0.00	0.00	0.00	0.00	0.00	0.00	0.00	0.00	0.00	0.00
	Right	0.00	0.00	0.00	0.00	0.00	0.00	0.00	0.00	0.00	0.00	0.00	0.00	0.00	0.00	0.00	0.00	0.00
WS	Left	0.00	0.00	0.00	0.00	0.00	0.00	0.00	0.00	0.00	0.00	0.00	0.00	0.00	0.00	0.00	0.00	0.00
	Right	0.00	0.00	0.00	0.00	0.00	0.00	0.00	0.00	0.00	0.00	0.00	0.00	0.00	0.00	0.00	0.00	0.00
HF	Left	0.00	0.00	0.00	0.00	0.00	0.00	0.00	0.00	0.00	0.00	0.00	0.00	0.00	0.00	0.00	0.00	0.00
	Right	0.00	0.00	0.00	0.00	0.00	0.00	0.00	0.00	0.00	0.00	0.00	0.00	0.00	0.00	0.00	0.00	0.00
HH	Left	0.00	0.00	0.00	0.00	0.00	0.00	0.00	0.00	0.00	0.00	0.00	0.00	0.00	0.00	0.00	0.00	0.00
	Right	0.00	0.00	0.00	0.00	0.00	0.00	0.00	0.00	0.00	0.00	0.00	0.00	0.00	0.00	0.00	0.00	0.00
UP	Left	0.00	0.00	0.00	0.00	0.00	0.00	0.00	0.00	0.00	0.00	0.00	0.00	0.00	0.00	0.00	0.00	0.00
	Right	0.00	0.00	0.00	0.00	0.00	0.00	0.00	0.00	0.00	0.00	0.00	0.00	0.00	0.00	0.00	0.00	0.00
EG	Left	0.00	0.00	0.00	0.00	0.00	0.00	0.00	0.00	0.00	0.00	0.00	0.00	0.00	0.00	0.00	0.00	0.00
	Right	0.00	0.00	0.00	0.00	0.00	0.00	0.00	0.00	0.00	0.00	0.00	0.00	0.00	0.00	0.00	0.00	0.00

Table S2. FA rate for left- and right-oriented fragments at each visual field location and for each BD for patients and controls. The table is complementary to Figure 4 and Figure S2. NaN – either no stimulus was presented at this location due to presentation randomization or the participant responded beyond the allocated time. NB: COI values could not be calculated with NaN values. For this reason, in Figure 4 and Figure S2 locations with NaN value are set to 0 (no COI effect).